Exp Brain Res (1999) 124:25–32

RESEARCH ARTICLE

T. Haslwanter · L.B Minor

Nystagmus induced by circular head shaking in normal human subjects

Received: 24 April 1997 / Accepted: 8 July 1998

Abstract We recorded three-dimensional eye and head movements during circular, horizontal, vertical, and torsional head shaking in six human subjects with normal vestibular function. With circular head shaking, the stimulation of the canals by the termination of the head movement is similar to that following a step in velocity about the naso-occipital axis. A large torsional nystagmus with slow phase eye velocity of about 20°/s was observed upon cessation of circular head shaking. The three-dimensional eye movements expected from stimulation of the semicircular canals by the head-shaking maneuvers were calculated. The predicted activation of the canals was determined by projecting the head velocity (in head coordinates) into the canal planes and then processing the signal with the transfer function of the canals. The torsional eye velocity components predicted by the stimulation of the canals matched the recorded ones. We observed small horizontal eye velocities that could not be predicted by the stimulation of the canals alone. No eye movements were observed after the end of head shaking about a fixed horizontal or vertical axis. The eye velocities following the termination of head oscillations in the roll plane were small. The analysis methods developed for this study may be useful in the investigation of eye movements elicited by other types of three-dimensional head movements.

Key words Eye movements · Active head movements · Three-dimensional · Semicircular canals · Vestibulo-ocular reflex

T. Haslwanter (✉)
Department of Neurology, University Hospital Tübingen, Hoppe-Seyler-Strasse 3, D-72076, Tübingen, Germany
e-mail: thomash@uni-tuebingen.de
Tel.: +49-7071-29-85661, Fax: +49-7071-29-5260

L.B Minor
Department of Otolaryngology, Head and Neck Surgery, School of Medicine, Johns Hopkins University, Baltimore, MD 21203-6402, USA

Introduction

Steps in angular head velocity about an earth-vertical axis evoke a horizontal nystagmus that declines in amplitude with a time constant determined by the mechanical properties of the semicircular canals and by velocity storage. A nystagmus with a similar time course, but oppositely directed, is noted at the termination of the rotation. These per- and postrotatory responses have been used to determine the dynamics of the horizontal vestibulo-ocular reflex (VOR) and to identify asymmetries in labyrinthine function. Such stimuli can be readily administered in the yaw plane with standard rotatory testing equipment. It has not been possible to produce comparable rotational stimuli in other planes with devices that are commonly available.

Recent studies have extended the types of rotational stimuli employed in investigations of vestibular function through the use of active head movements (Tomlinson et al. 1980; Fineberg et al. 1987; O'Leary and Davis 1990; O'Leary et al. 1991; Meulenbroeks et al. 1995; Nagayama et al. 1995). These studies have increased the range of frequencies accessible to experimental investigation and also allowed testing of the properties of the vertical VOR (Demer and Viirre 1996). Since head rotations were not recorded in all three dimensions, it has not been possible to determine the stimulation of individual semicircular canals. Limitations in eye and head movement recording techniques and in the methods of analysis have restricted these experiments to rotations about a single, fixed axis.

Nystagmus following head shaking about a fixed horizontal or vertical axis is commonly seen in patients with unilateral vestibular hypofunction (Hain et al. 1987; Fetter et al. 1990; Jacobson et al. 1990). Such responses have been interpreted as the effect of asymmetric inputs from the intact labyrinth, due to the range of excitation being higher than that for inhibition, perseverated by central velocity storage mechanisms. Such nystagmus is therefore not observed in subjects with symmetrical vestibular function. Hain and Spindler (1993) noted a tor-

Table 1 Characteristics of the clockwise (*CW*), counterclockwise (*CCW*), horizontal, vertical, and torsional head-shaking maneuvers: means±SD of the six subjects; *Range* indicates the total range of the head oscillation (peak-to-peak)

	CW	CCW	Hor	Ver	Tor
No. of cycles	23±7	22±6	24±7	23±7	21±8
Range (°)	88±16	89±21	74±22	43±16	66±10
Frequency (cycles/s)	1.3±0.3	1.3±0.4	1.9±0.3	1.9±0.3	1.2±0.3
Max. velocity (°/s)	406±137	425±143	454±138	295±87	331±89

sional nystagmus following circular head shaking that included combined horizontal and vertical components in subjects with presumed normal vestibular function. The mechanism of this nystagmus was not defined.

The aim of this study was to evaluate the nystagmus evoked by circular head shaking in terms of the effects of the head movement on the semicircular canals. To accomplish this goal, we developed an algorithm to determine the magnitude of the stimulation of the six canals as a function of the head velocity stimulus. We found that the stimulus elicited by abrupt termination of circular head shaking is similar to a step of head velocity about the naso-occipital axis. We showed that the eye velocities predicted solely by the stimulation of the six canals match the observed torsional components of the nystagmus.

Methods

We recorded three-dimensional eye movements during horizontal, vertical, torsional, and circular head shaking. Recordings were made at the institutions of the two authors on different experimental rigs. Subjects gave informed consent for the recordings which were performed in accordance with protocols approved by the respective institutional ethics committees. Analysis of the findings showed no difference between the data acquired at the two locations. In the following description the locations are referred to as location A and location B when differences need to be defined.

Subjects

The experiments were performed in six subjects with no known deficits in vestibular function and normal vestibulo-ocular examinations. The subjects ranged in age from 29 to 40 years.

Eye and head position recording

The dual search coil technique was used to record three-dimensional eye position. The search coils were manufactured by Skalar (Delft, Netherlands). In location A, the magnetic field was produced by three orthogonal pairs of coils with a diameter and a distance of 1.4 m, and was such that the head of the subject was exactly in the center of the magnetic fields. Signals from all three fields were recorded, and the system was automatically calibrated at the beginning of the experiments (Bechert and Koenig 1996). Data were sampled at 100 Hz, and the reference position was taken from the beginning or the end of the recording when the subject was looking at a fixation light located straight ahead. A search coil mounted on a bite bar was used to record head position. To facilitate fixation of the bite-bar, a layer of thermoplastic material was heated before the experiment, molded around the bite-bar, and placed in the subject's mouth for a dental impression.

In location B, the head was centered in a cube-shaped, 100-cm aluminum frame in which three magnetic fields with different frequencies were generated. Details of the eye coil calibration have been published previously (Straumann et al. 1995). Signals from all three orthogonal magnetic fields were sampled at 500 Hz.

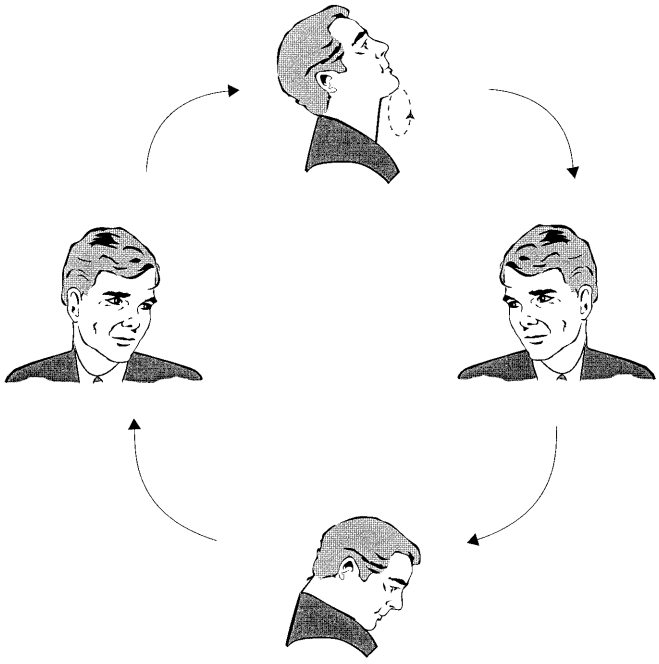

Fig. 1 Sketch of CW head shaking. *Solid arrows* Direction of head movement; *dashed loop (top picture)* motion of the chin during this stimulus

Paradigm

Subjects were seated upright inside the magnetic field. The head was kept in a comfortable orientation, and the inclination of Reid's line (i.e., the line between the lower rim of the orbits and the center of the external acoustic meatus) relative to the earth-horizontal plane was measured with a goniometer. Reid's line was tilted between 10° and 20° nose-up at the beginning of each rotational stimulus. The subjects were asked to fixate a reference target that was presented for a few seconds. After the light was turned off, subjects began to move their head sinusoidally at their own pace in one of five different directions: horizontal ("no" shaking), vertical ("yes" shaking), torsional (head to the right and left shoulder), clockwise (CW, "up–right–down–left") or counterclockwise (CCW, "up–left–down–right").

The execution of a head-shaking maneuver in the CW direction is illustrated in Fig. 1. Subjects were told to imagine a circular loop in front of their face (Fig. 1, top), and to trace this loop with their chin while keeping their eyes shut. Immediately after the end of the head shaking, they were asked to open the eyes and look straight ahead in the dark.

Table 1 lists the characteristics of the head-shaking maneuvers.

Data analysis

Since the head-shaking maneuvers were active, they were executed differently by each subject. To determine the amount of vestibular stimulation induced by the individual head movements we proceeded as follows:

The reference position for eye and head movements was taken from the initial period of the data acquisition, where the head was stationary and the subject was fixating the reference target light. Eye-in-space and head positions were then expressed as quaternions, describing the rotation with respect to this reference position. From the quaternions describing the orientation of eye-in-space (q_{es}) and the ones describing head-in-space (q_{hs}), the orientation of the eye-in-head (q_{eh}) was calculated as:

$$q_{eh} = q^{-1}{}_{hs} \bullet q_{es} \quad (1)$$

where "•" indicates a quaternion multiplication (Tweed et al. 1990). Three-dimensional head velocity was calculated from head position and its time derivative. The time derivative was determined with a Savitzky-Golay filter, using a second-order polynomial, and considering five data points before and after each point (Savitzky and Golay 1964; Press et al. 1992). Eye-in-head velocity in three dimensions was determined in an analogous way. Data were desaccaded since only the velocity of the slow-phase components of nystagmus was required for further analysis. The fast phases of the nystagmus were removed by grouping data into bins of 100 data points each, and calculating the median for each bin. Neighboring bins were overlapping, staggered by five data points. While this reduction in sampling rate to 20 Hz may suggest a very strong filtering of the data, visual inspection of each desaccaded data trace confirmed that this setting led to a reliable desaccading of the data, without any loss of information important for the analysis.[1]

To determine the actual stimulation of the canals and the eye movement response expected from this stimulation, we performed the following six steps for the analysis[2]:

1. We first determined the head velocity in space coordinates, $\underline{\omega}^{h}{}_{sc,}$ measured directly from the data.
2. We projected the head-velocity vector into the canal planes in order to find the angular velocity "seen" by each canal ($\underline{\omega}^{h}{}_{cc}$, the angular velocity expressed in canal coordinates). This was carried out by multiplying $\underline{\omega}^{h}{}_{sc}$ by the 3×3 matrix $\mathbf{C}_{scc,}$ whose rows were normalized vectors perpendicular to the canal planes:

   $$\underline{\omega}^{h}{}_{cc} = \mathbf{C}_{scc} * \underline{\omega}^{h}{}_{sc} \quad (2)$$

   where "*" indicates a vector or matrix multiplication. The orientation of the head in space and the orientation of the canals with respect to the stereotaxic coordinate system (Blanks et al. 1975) were used to calculate $\mathbf{C}_{scc}$. Replacing $\mathbf{C}_{scc}$ by $\mathbf{C}_{head}$, the rotation matrix describing the current position of the head, provided the head velocity expressed in a head-fixed coordinate system, $\underline{\omega}^{h}{}_{hc}$. Since we assumed the same dynamic behavior for the horizontal, anterior, and posterior canals, the predicted eye velocity was not affected by our choice of $\mathbf{C}_{scc}$ over $\mathbf{C}_{head}$.
3. The semicircular canals act as a high-pass filter, with a time constant that has been estimated to be about 7 s in humans. The signal in the vestibular afferents $\underline{v}_{aff}$ was obtained by passing the head velocity $\underline{\omega}^{h}{}_{cc}$ through this high-pass filter. In Laplace notation this can be written as:

   $$\underline{v}_{aff} = \frac{s}{7s+1} \cdot \underline{\omega}^{h}{}_{cc} \quad (3)$$

   where "·" denotes a scalar multiplication.
4. The eye movements corresponding to these canal signals were reconstructed by multiplying $\underline{v}_{aff}$ with the inverse of the canal matrix:

   $$\underline{\omega}^{e}{}_{hc} = \mathbf{C}^{-1}{}_{scc} * \underline{v}_{aff} \quad (4)$$

   For this computation we assumed that the processing of the canal signals by the brainstem and eye muscles resulted in an eye velocity aligned exactly with the head velocity.
5. Since three-dimensional gain values had not previously been determined for oculomotor responses in humans at the frequencies used in this experiment, the gain values for the horizontal, vertical, and torsional components were measured from the maximum eye velocity responses during the head oscillations in these planes (0.45, 0.57, and 0.24 for the horizontal, vertical, and torsional components, respectively). The ratios between the horizontal, vertical, and torsional gain components were similar to those obtained by Tweed et al. (1994b). They recorded horizontal, vertical, and torsional gain values at 0.3 Hz of 0.66, 0.74, and 0.39, respectively. The reduced gains in our experiments may be caused by the fact that our subjects were given no fixation instructions during the head-shaking maneuvers.
6. We added velocity storage to the horizontal eye movement component, which extended the time constant of the response to a velocity step to 14 s. The velocity storage for the vertical and torsional eye velocity components has been determined to be negligible (Tweed et al. 1994a). In the following we refer to the resulting eye velocity as $\underline{\omega}^{e}{}_{exp}$, the "expected" eye velocity. Note that $\underline{\omega}^{e}{}_{exp}$ is in head coordinates, not in space coordinates.

This analysis procedure yielded an *expected three-dimensional eye velocity* for each subject, which was based purely on the stimulation of the semicircular canals by the head movements. Comparing the magnitude of this expected response with the one actually recorded, we obtained the *gain*:

$$\text{gain} = |\underline{\omega}^{e}{}_{hc}| / |\underline{\omega}^{e}{}_{exp}| \quad (5)$$

[1] A similar method of desaccading eye velocity data has been described in detail by Straumann (1991).

[2] For mathematical quantities we use the following notation: all vectors are underlined (e.g., $\underline{\omega}$); matrices are boldfaced (e.g., $\mathbf{C}$); and scalar quantities and quaternions are written in plain style (e.g., gain).

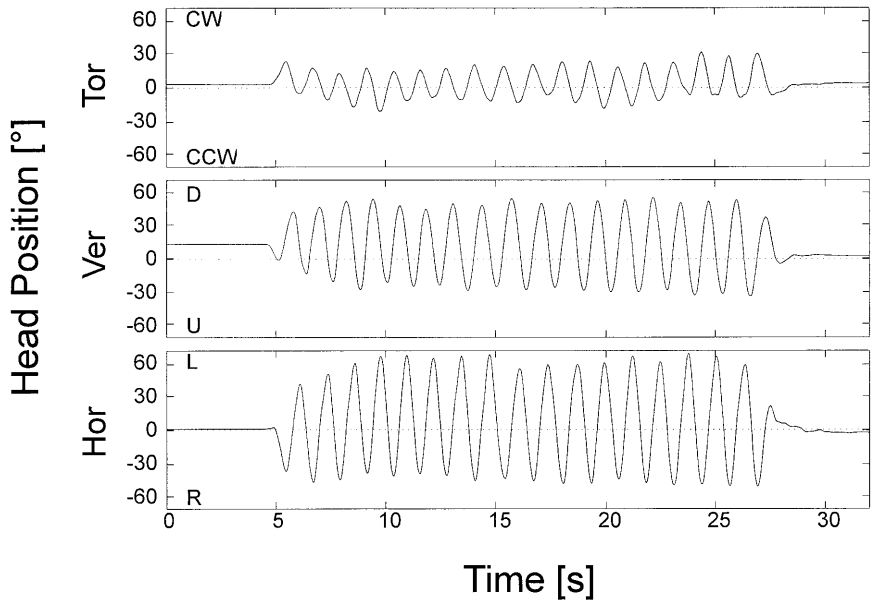

Fig. 2 Torsional, vertical, and horizontal head position during CW head shaking

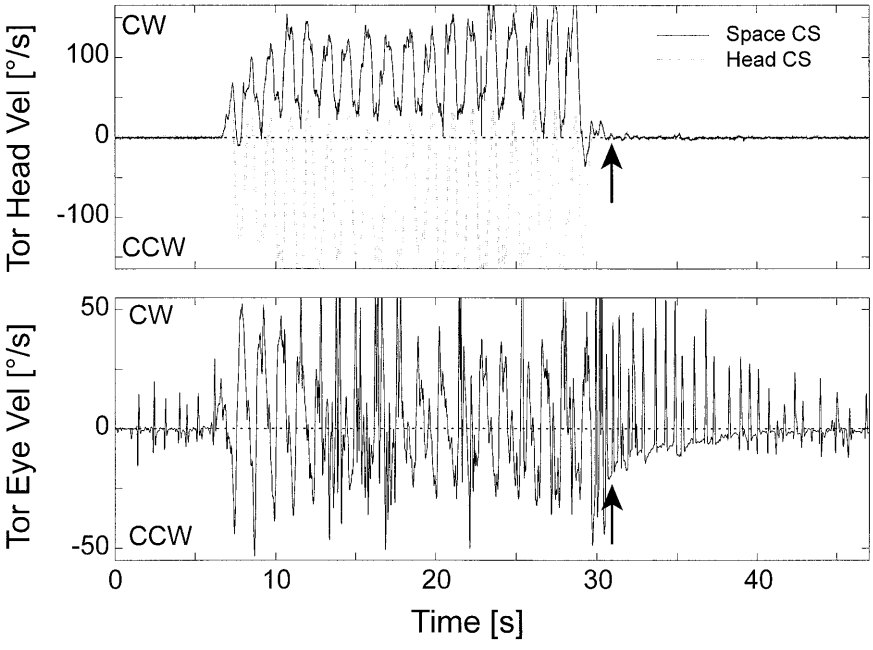

Fig. 3 *Above* Torsional head velocity during the CW head shaking shown in Fig. 2. *Arrows* End of the head shaking; *solid black line*, torsional component of $\underline{\omega}^{h}_{sc}$, the head velocity in space coordinates; *dashed gray line* torsional component of $\underline{\omega}^{h}_{hc}$, the head velocity expressed in a head-fixed coordinate system. *Below* Corresponding torsional eye velocity components, expressed with respect to the head

where "| |" indicates the length of the vector. Since the length of a vector does not define its orientation, we also calculated the angle between the recorded and the predicted response:

$$\text{angle} = \text{acos}\left(\frac{\underline{\omega}^{e}_{exp} * \underline{\omega}^{e}_{hc}}{|\underline{\omega}^{e}_{exp}| \cdot |\underline{\omega}^{e}_{hc}|}\right) \quad (6)$$

Gain and angle were not calculated for $|\underline{\omega}^{e}_{exp}|$ smaller than 2°/s, since division by small numbers can lead to spurious results.

Finally, we determined the difference between the expected and the recorded response:

$$\underline{\omega}^{diff} = \underline{\omega}^{e}_{hc} - \underline{\omega}^{e}_{exp} \quad (7)$$

These procedures were applied to all directions of head shaking (horizontal, vertical, torsional, CW, and CCW).

For averaging the data from different subjects, the end of the head movement was defined as the last moment when the total head velocity exceeded 20°/s. The traces from different individuals were superimposed so that the end of the head movements coincided.

Results

Subjects had no difficulty performing the circular head shaking, but reported an illusion of circular vection following the head shaking. The torsional head movement

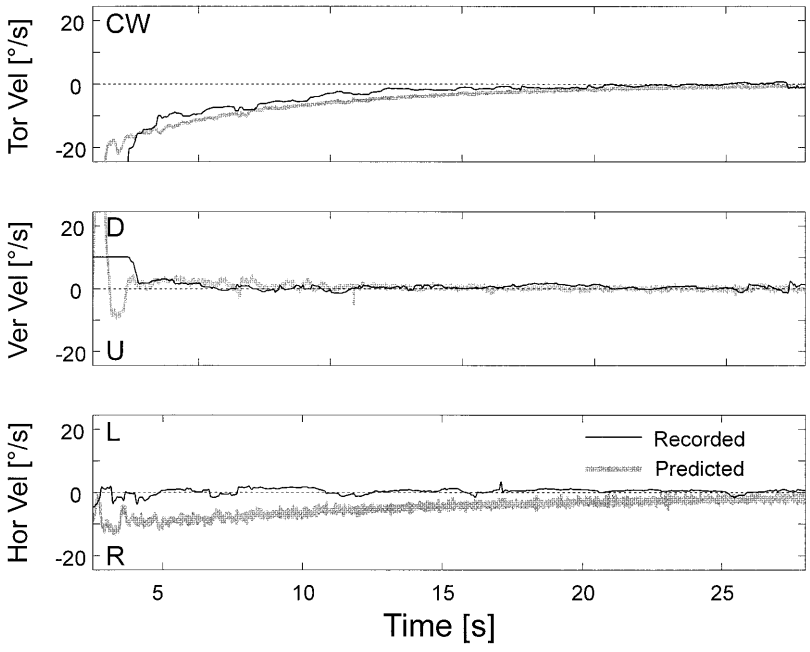

Fig. 4 Torsional, vertical, and horizontal components of the desaccaded eye velocity traces (*thin black line*), and the eye velocity components predicted from the stimulation of the canals (*thick gray line*). Same data as in Figs. 2 and 3

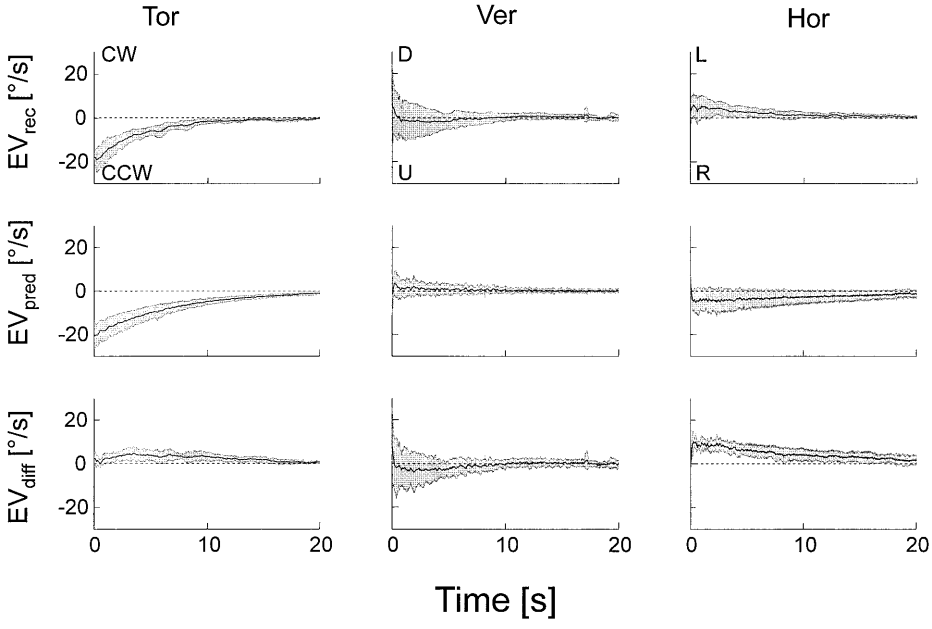

Fig. 5 Means and standard deviations of the eye velocity following CW head shaking. *Upper row* Recorded eye velocity traces; *middle row* predicted eye velocity traces; *bottom row* difference between recorded and predicted eye velocities. For each row, *columns* represent torsional, vertical, and horizontal eye velocity components (*left to right*)

during the circular head shaking was smaller than the horizontal and the vertical components. Figure 2 shows torsional, vertical and horizontal head position data from one subject.

The solid trace on the top of Fig. 3 represents the corresponding head velocity. The mechanical constraints imposed by fixation of the head on the neck restricted torsional head position to values around 0°. For circular head movements in the CW direction this constraint led to a head velocity bias for the torsional component. In space coordinates this bias was CW, whereas in head coordinates it was CCW (Fig. 3, solid and dashed trace, respectively). Head velocity expressed in head coordinates determined the stimulation of the canals.

Abrupt termination of the head movement by the subject, at around 31 s, elicited eye movements with slow phases in the CCW direction (Fig. 3, bottom), the same direction as the preceding bias component of torsional head velocity. This postrotatory nystagmus is analogous to the nystagmus with leftward slow phase components that follows termination of a leftward rotation.

The corresponding desaccaded eye velocity traces as well as the eye velocity components predicted from the stimulation of the canals (described in “Methods”) are shown in Fig. 4. The torsional eye velocity components were in agreement with those predicted by the mechanical stimulation of the canals, without requiring any further processing of the signals. In contrast, we did not ob-

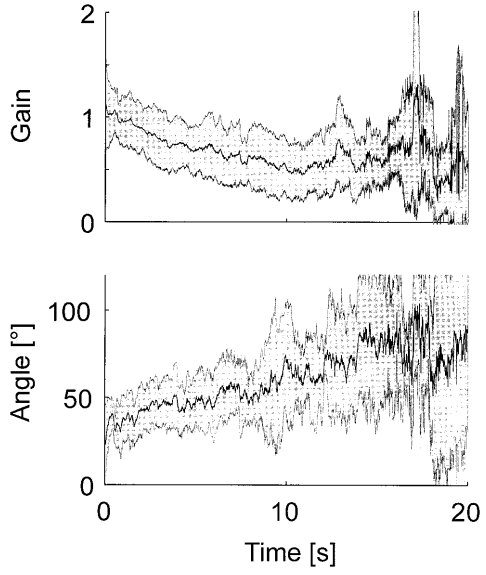

Fig. 6 Gains and angles between the recorded eye velocity $\underline{\omega}^{e}_{hc}$ and the expected eye velocity $\underline{\omega}^{e}_{exp}$, following circular head shaking in the CW direction

serve a horizontal eye velocity component although a rightward slow phase component was predicted.

Means and standard deviations of the eye velocity responses to head shaking in the CW direction from all subjects are presented in Fig. 5. The top, middle, and bottom rows show the recorded eye velocities, the eye velocities predicted from the stimulation of the semicircular canals, and the difference between the two (recorded minus predicted), respectively.

Averaging the eye velocities over the first 0.5 s gave an initial torsional response of –18.5±4.9°/s (mean±SD). Our model (described in "Methods") predicted a response of –18.4±6.9°/s. The variability in these responses arose from the individual variations in the execution of the head movement.

The observed torsional response decayed with a time constant of only 3.9 s, shorter than the 7 s time constant used to describe the mechanical properties of the canals.

The discrepancy between observed and predicted horizontal eye movements, as shown in Fig. 4, occurred systematically in all subjects. While the model predicted slow phases to the right, the observed eye velocity components tended to have slow phases to the left (Fig. 5, right column). The initial difference between the recorded and the predicted horizontal eye velocities is 8.4±3.6°/s. Changing the time constant of velocity storage in the model did not change this prediction.

The fast decay of the recorded eye velocity caused the gain (recorded total eye velocity/predicted total eye velocity) to decrease with time (Fig. 6, top). At the same time, the angle between the recorded and the predicted eye velocity gradually increased (from 39±13° to 76±30° at 1 and 10 s after the end of head shaking, respectively; Fig. 6, bottom). This increase was due mainly to an increased alignment of the eye velocity axis with the earth-vertical axis for circular head shaking in the CW direction, but a similar increase in the misalignment following head shaking in the CCW direction (from 30±6° to 65±30°) was nonspecific. The findings were otherwise similar for CCW head shaking: the initial torsional eye velocity was 16.3±9.5°/s, whereas the predicted response was 18.2±5.8°/s; the recorded eye velocity decayed with a time constant of 3.7 s; and the difference between recorded and predicted eye velocity was –5.7±4.3°/s (i.e., in this case the recorded horizontal eye velocity tended to have slow phases to the right, whereas the model predicted slow phases to the left).

As expected, horizontal and vertical head shaking induced no consistent nystagmus in our group of subjects with normal vestibular function (Hain and Spindler 1993). The head movements during torsional head shaking were such that, based upon our model, we would have expected eye movements with slow phases directed slightly upward (–5.5±6.6°/s). The observed vertical eye movements were indeed upward, but usually smaller than expected (–2.3±5.3°/s). Eye movements in the torsional and horizontal direction were uneventful.

Discussion

Why does our circular head-shaking paradigm induce postrotatory nystagmus in normal subjects? The circular head motion includes a sustained torsional velocity, as shown in Fig. 3, and its cessation therefore evokes torsional slow phases in the same direction, just as stopping a constant velocity roll motion would do. In most subjects this nystagmus is also associated with an illusion of circular vection.

In Fig. 3, the subject maintained an average torsional velocity of about 85°/s CW for over 20 s. That his head position did not twist but stayed near 0° torsion is a surprising consequence of three-dimensional kinematics. This effect is not specific to torsion: other complex multi-axis head movements can contain effective constant velocity yaw and pitch components, although such movements were not investigated here. To execute a circular, horizontal-vertical head movement (e.g., CW=up–right–down–left) with constant zero torsional position, the head velocity vector $\underline{\omega}^{h}$ must trace a cone-shaped path as shown in Fig. 7A (Tweed et al. 1990).

Figure 7B presents a snapshot of that movement, in the head-up position. If the torsional head position is to remain zero, the head velocity vector $\underline{\omega}^{h}$ must tilt half as far back from the vertical plane as the head[3]. For eye movements the same property is referred to as the "half-angle rule" (Misslisch et al. 1994). Projecting $\underline{\omega}^{h}$ from Fig. 7B onto the space-fixed torsional axis (tor_{space} in Fig. 7C, solid lines) gives a positive (CW) torsional component, which corresponds to the CW bias velocity

[3] A circular head movement with exactly zero torsional position, described by the quaternion vector $q=\alpha^*[0, \sin(\omega t), \cos(\omega t)]$, corresponds to the angular velocity $\omega^{h}_{sc} = \alpha\ \omega^* [\alpha, \mathrm{sqrt}(1-\alpha^2)*\cos(\omega t), -\mathrm{sqrt}(1-\alpha^2)*\sin(\omega t)$. Note the constant, nonzero torsional velocity.

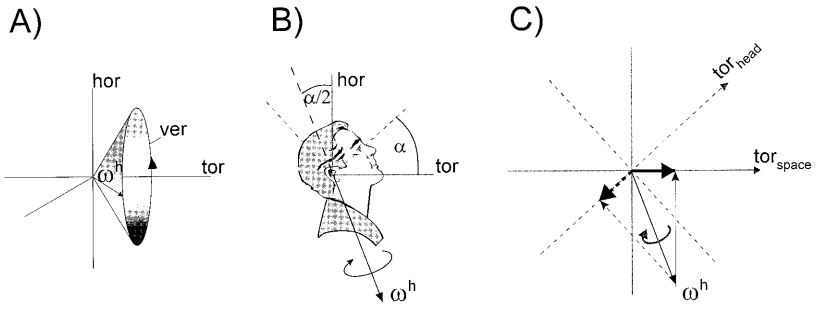

Fig. 7 **A** During circular head shaking in the CW direction, the angular head-velocity vector, $\underline{\omega}^h$, traces an approximately cone-shaped path. **B** Snapshot of the movement, while the head is "up." To keep the head close to the zero-torsion position, $\underline{\omega}^h$ is tilted only half as far ($\alpha/2$) as the head (α). **C** Consequently, projection of $\underline{\omega}^h$ onto the space-fixed torsional axis gives a positive torsional component (*solid lines*), but projection onto the head-fixed torsional axis gives a negative torsional component (*dashed lines*)

in Fig. 3. Projecting the same $\underline{\omega}^h$ onto the head-fixed torsional axis (tor_{head}, dashed lines) gives a negative (CCW) torsional bias velocity, corresponding to the negative bias of the dashed line in Fig. 3. Since in our recorded data the head position is not zero but modulated about zero (Fig. 2), this bias is superimposed on the velocity modulation observed in Fig. 3.

Termination of CW head shaking excites the three semicircular canals on the right and inhibits those on the left (Aw et al. 1996). The reverse is true for cessation of CCW head shaking. The amount of canal stimulation is proportional to the frequency of the oscillation and to the square of the radius of the head movement. Using the technique described in "Methods," we calculated the exact canal stimulation evoked by these complex head movements. The predicted postrotatory torsional eye velocity matched the recorded one. It decayed with a time constant of only 3.8 s which is probably shorter than the time constant of the canals, although this value is not known with certainty in humans. The reduction in the time constant might be caused by the mismatch between the canal signal, which still indicates a rotation about the torsional axis, and the otolith information, which signals a stable orientation in space. This hypothesis is supported by simulations of the otolith contribution to the eye movements elicited by circular head shaking, which we made with a model originally developed to mimic otolith-canal interaction during off-vertical axis rotation. The results of this simulation, based on ideas by Merfeld (1995), indicate that the otolith contributions probably cause the observed reduction in the torsional time constant. However, these simulations suggest that the contributions of the otoliths are too small to explain the discrepancy between the horizontal component of the recorded and predicted eye movements. As shown in Fig. 5 (right column), the predicted horizontal nystagmus following CW head shaking had predominantly slow phases to the right, whereas the recorded slow phases were to the left. These unexplained velocity components might be caused by involvement of signals from the cervical afferents (Doerr et al. 1984), but further experimental investigations would be needed to clarify this issue. We also were unable to establish a correlation between the recorded mismatch and any of the parameters describing the execution of the head shaking such as movement amplitude and asymmetries during the circular head movement.

The velocity-storage mechanism that was included in our model of the processing of vestibular signals for the horizontal direction did not appear to contribute significantly to the eye movements. Velocity storage increases the time constant of the horizontal nystagmus beyond the peripheral time constant of the semicircular canals. In our experiments, however, the horizontal eye velocity decayed approximately with the time constant of the canals (5.7 s for CW head shaking, and 8.6 s for CCW).

The mechanism through which eye movements are elicited following circular head shaking is fundamentally different from that responsible for the nystagmus after head shaking about a fixed axis. Responses to horizontal and vertical head shaking have been used to detect pathologies in vestibulo-ocular pathways (Hain et al. 1987; Fetter et al. 1990; Jacobson et al. 1990). Sustained head shaking about a fixed axis in normal subjects does not induce nystagmus after an abrupt termination, since the vestibular activity elicited by the rotation in one direction is immediately canceled by the following rotation in the opposite direction. Asymmetry in the system is required to elicit nystagmus following horizontal or vertical head shaking. This asymmetry can have a peripheral cause, such as vestibular neurectomy, or can be found at a more central level, for example in brainstem lesions (Hain and Spindler 1993). In contrast, when the axis of head velocity is changed continuously, the canals experience a stimulation at least along one axis that is similar to the one elicited by a velocity step on a turntable (note the torsional velocity bias in Fig. 3).

The methods used in this study to predict canal-evoked nystagmus are generally applicable to investigations of the relationship between three-dimensional eye and head movements. Previous efforts to record eye movements evoked by active head movements were often aimed at extending the frequency range of the investigations, and/or at testing vestibular function without an expensive rotating chair (Meulenbroeks et al. 1995; Fineberg et al. 1987; O'Leary and Davis 1990; Nagayama et al. 1995; Tomlinson et al. 1980; O'Leary et al. 1991). All of these experiments were restricted to a fixed

axis of rotation or at most to combined horizontal/vertical eye and head rotations. The present study shows that vestibulo-ocular responses to more complex head movements can be recorded and interpreted on the basis of geometric principles relating characteristics of the head movement stimulus and eye movement response. The circular head-shaking stimulus delivers a velocity step in torsion without the requirement of a mechanical turntable. Responses to this stimulus may therefore be useful in the identification of unilateral or bilateral vestibular hypofunction.

Acknowledgements This work was supported by Deutsche Forschungsgemeinschaft SFB 307-A10, NIH R01 DC 02390 and P60 DC 00979, and by the National Space Biomedical Research Institute. We also want to thank D. Tweed for his careful reading of the manuscript.

References

Aw ST, Halmagyi GM, Haslwanter T, Curthoys IS, Yavor RA, Todd MJ (1996) Three-dimensional vector analysis of the human vestibuloocular reflex in response to high-acceleration head rotations II. Responses in subjects with unilateral vestibular loss and selective semicircular canal occlusion. J Neurophysiol 76:4021–4030

Bechert K, Koenig E (1996) A search coil system with automatic field stabilization, calibration, and geometric processing for eye movement recording in humans. Neuroophthalmology 16: 163–170

Blanks RHI, Curthoys IS, Markham CH (1975) Planar Relationships of the Semicircular Canals in Man. Acta Otolaryngol (Stockh) 80:185–196

Demer JL, Viirre ES (1996) Visual-vestibular interaction during standing, walking, and running. J Vestib Res 6:295–313

Doerr M, Hong SH, Thoden U (1984) Eye movements during active head turning with different vestibular and cervical input. Acta Otolaryngol (Stockh) 98:14–20

Fetter M, Zee DS, Koenig E, Dichgans J (1990) Head shaking nystagmus during vestibular compensation in humans and rhesus monkeys. Acta Otolaryngol (Stockh) 110:175–181

Fineberg R, O'Leary DP, Davis LL (1987) Use of active head movements for computerized vestibular testing. Arch Otolaryngol Head Neck Surg 113:1063–1065

Hain TC, Spindler J (1993) Head-shaking nystagmus. In: Sharpe JA, Barber HO (eds) The vestibulo-ocular reflex and vertigo. Raven Press, New York, pp 217–228

Hain TC, Fetter M, Zee DS (1987) Head-Shaking Nystagmus in Patients with Unilateral Peripheral Vestibular Lesions. Am J Otolaryngol 8:36–47

Jacobson GP, Newman CW, Safadi I (1990) Sensitivity and specificity of the headshaking test for detecting vestibular system abnormalities. Ann Otol Rhinol Laryngol 99:539–542

Merfeld DM (1995) Modeling human vestibular responses during eccentric rotation and off vertical axis rotation. Acta Otolaryngol Suppl (Stockh) 520:354–359

Meulenbroeks AAWM, Kingma H, van Twisk JJ, Vermeulen MP (1995) Quantitative evaluation of the vestibular autorotation test (VAT) in normal subjects. Acta Otolaryngol Suppl (Stockh) 520:327–333

Misslisch H, Tweed D, Fetter M, Sievering D, Koenig E (1994) Rotational kinematics of the human vestibuloocular reflex III. Listing's law. J Neurophysiol 72:2490–2502

Nagayama I, Kato H, Okabe Y, Furukawa M (1995) Development of high frequency vestibulo-ocular responses to active head shaking. Acta Otolaryngol Suppl (Stockh) 519:265–267

O'Leary DP, Davis LL (1990) High-frequency autorotational testing of the vestibulo-ocular reflex. Neurol Clin 8:297–312

O'Leary DP, Davis LL, Maceri DR (1991) Vestibular autorotation test asymmetry analaysis of acoustic neuroma. Otolaryngol Head Neck Surg 104:103–109

Press WH, Teukolsky SA, Vetterling WT, Flannery SA (1992) Numerical recipes in C, 2nd edn. Cambridge University Press, Cambridge

Savitzky A, Golay MJE (1964) Smoothing and differentiation of data by simplified least squares procedures. Anal Chem 36:1627–1639

Straumann D (1991) Off-line computing of slow-phase eye velocity profiles evoked by velocity steps or caloric stimulation. Int J Biomed Comput 29:61–65

Straumann D, Zee DS, Solomon D, Lasker AG, Roberts DC (1995) Transient torsion during and after saccades. Vision Res 35:3321–3334

Tomlinson RD, Saunders GE, Schwarz DWF (1980) Analysis of human vestibulo-ocular reflex during active head movements. Acta Otolaryngol (Stockh) 90:184–190

Tweed D, Cadera W, Vilis T (1990) Computing three-dimensional eye position quaternions and eye velocity from search coil signals. Vision Res 30:97–110

Tweed D, Fetter M, Sievering D, Misslisch H, Koenig E (1994a) Rotational kinematics of the human vestibuloocular reflex II. Velocity steps. J Neurophysiol 72:2480–2489

Tweed D, Sievering D, Misslisch H, Fetter M, Zee D, Koenig E (1994b) Rotational kinematics of the human vestibuloocular reflex I. Gain matrices. J Neurophysiol 72:2467–2479